journal of the mechanical behavior of biomedical materials 152 (2024) 106433

Contents lists available at ScienceDirect

Journal of the Mechanical Behavior of Biomedical Materials

journal homepage: www.elsevier.com/locate/jmbbm

Fabrication and biomechanical characterization of a spider silk reinforced fibrin-based vascular prosthesis

Clara Glomb [a], Mathias Wilhelmi [a,b], Sarah Strauß [c], Sarah Zippusch [a,d], Melanie Klingenberg [a,d], Thomas Aper [a,d], Peter M. Vogt [c], Arjang Ruhparwar [a,d], Florian Helms [a,d,*]

[a] Lower Saxony Centre for Biomedical Engineering, Implant Research and Development (NIFE), Hannover Medical School, Stadtfelddamm 34, 30625, Hannover, Germany
[b] Department of Vascular- and Endovascular Surgery, St. Bernward Hospital, Hildesheim, Germany
[c] Department of Plastic, Hand and Reconstructive Surgery, Hannover Medical School, Carl-Neuberg-Strasse 1, 30625, Hannover, Germany
[d] Division for Cardiothoracic-, Transplantation- and Vascular Surgery, Hannover Medical School, Hannover, Germany

ARTICLE INFO

Keywords:
Tissue engineering
Vascular grafts
Spider silk reinforcement

ABSTRACT

With fibrin-based vascular prostheses, vascular tissue engineering offers a promising approach for the fabrication of biologically active regenerative vascular grafts. As a potentially autologous biomaterial, fibrin exhibits excellent hemo- and biocompatibility. However, the major problem in the use of fibrin constructs in vascular tissue engineering, which has so far prevented their widespread clinical application, is the insufficient biomechanical stability of unprocessed fibrin matrices.

In this proof-of-concept study, we investigated to what extent the addition of a spider silk network into the wall structure of fibrin-based vascular prostheses leads to an increase in biomechanical stability and an improvement in the biomimetic elastic behavior of the grafts. For the fabrication of hybrid prostheses composed of fibrin and spider silk, a statically cast tubular fibrin matrix was surrounded with an envelope layer of *Trichonephila edulis* silk using a custom built coiling machine. The fibrin matrix was then compacted and pressed into the spider silk network by transluminal balloon compression.

This manufacturing process resulted in a hybrid prosthesis with a luminal diameter of 4 mm. Biomechanical characterization revealed a significant increase in biomechanical stability of spider silk reinforced grafts compared to exclusively compacted fibrin segments with a mean burst pressure of 362 ± 74 mmHg vs. 213 ± 14 mmHg ($p < 0.05$). Dynamic elastic behavior of the spider silk reinforced grafts was similar to native arteries. In addition, the coiling with spider silk allowed a significant increase in suture retention strength and resistance to external compression without compromising the endothelialization capacity of the grafts.

Thus, spider silk reinforcement using the abluminal coiling technique represents an efficient and reproducible technique to optimize the biomechanical behavior of small-diameter fibrin-based vascular grafts.

1. Introduction

Cardiovascular diseases are the number one cause of death worldwide (Dicker et al., 2018). Therapeutic strategies often require surgical replacement of stenotic, occluded, or damaged blood vessels using vascular prostheses. However, long-term outcomes of currently available vascular prostheses are limited due to insufficient hemo- and biocompatibility of synthetic graft materials like expanded polytetrafluorethylene (ePTFE) or polyethylene terephthalate (Dacron®), which still today represent the gold standard for prosthetic vascular replacement (Formichi et al., 1988; Greisler et al., 1986; Roll et al., 2008). On the other hand, the use of autologous blood vessels for vessel replacement is limited by inconsistent graft availability and quality (Tu et al., 1997). Consequently, there is a great clinical need for innovative blood vessel substitutes with *off the shelf* availability and superior hemo- and biocompatibility compared to currently available synthetic graft materials.

To achieve these goals, vascular tissue engineering targets to

* Corresponding author. Hannover Medical School, Division for Cardiothoracic-, Transplantation- and Vascular Surgery, Carl-Neuberg-Str. 1, 30625, Hannover, Germany.
E-mail address: helms.florian@mh-hannover.de (F. Helms).

https://doi.org/10.1016/j.jmbbm.2024.106433
Received 3 December 2023; Received in revised form 15 January 2024; Accepted 25 January 2024
Available online 1 February 2024

generate biologically active vascular prostheses which facilitate integration into the target organism and show high regenerative potential. As a particularly promising regenerative matrix material, fibrin is currently used in various tissue engineering approaches (Shaikh et al., 2008). Over the last decade, fibrin has gained popularity as a matrix material for vascular tissue engineering as well due to its excellent hemo- and biocompatibility (Shaikh et al., 2008; Gui et al., 2014; Wilhelmi et al., 2014). Its function as a cell-carrier for all cell types relevant for vascular tissue engineering has been proven (Helms et al., 2021a) and biocompatibility has been confirmed in long-term clinical human application in the form of fibrin-based adhesives for adjuvant hemostasis in cardiovascular surgery (Rousou, 2013). This unique combination of autologous availability, ease of processing, high regenerative potential and already clinically proven hemo- and biocompatibility makes fibrin a nearly ideal matrix material for vascular tissue engineering applications. The last major hurdle for the broad clinical application of fibrin-based bioartificial vascular prostheses is the still insufficient biomechanical stability of unprocessed fibrin matrices, which is currently the subject of intensive research. We and other groups have developed various approaches to stabilize fibrin matrices, ranging from modifications during the casting process (Helms et al., 2020) to different strategies for matrix compaction (Aper et al., 2016, 2018) and the use of hybrid polymers (Wilhelmi et al., 2014) to *in vitro* cell colonization with formation of collagen-rich extracellular matrices (Gui et al., 2014). In our previous work, we showed that in particular transluminal balloon compression contributes to efficient fibrin matrix compaction and increased biomechanical stability of tubular fibrin constructs (Helms et al., 2021b). All these methods, each with their own advantages and disadvantages, have already led to distinct improvement in the mechanical stability of fibrin-based vascular prostheses. However, fibrin grafts that provide sufficient biomechanical stability not only to withstand physiological and supraphysiological blood pressures after implantation *in vivo*, but also allow surgical handling with sufficient suturability and reliable structural integrity sufficient for clinical applications have not been generated to date.

A recently established approach to achieve the desired biomechanical stability in fibrin-based implants is the combination of a fibrin matrix and a spider silk scaffold, which we described first for fibrin-based cardiac patches (Bobylev et al., 2022). Spider silk has unique biomechanical and biological properties, which is why it has recently found increasing use in various areas of tissue engineering. The dragline silk is characterized on the one hand by extreme tensile strength with simultaneous stretchability at minimal diameter (Hennecke et al., 2013; Kuhbier et al., 2011), while on the other hand spider silk is bio- and hemocompatible and resorbable as well (Allmeling et al., 2008a; Kuhbier et al., 2017a; Liebsch et al., 2018; Radtke et al., 2011). This makes it particularly suitable for applications where a transient lead structure is required in the context of in situ tissue engineering (Strauβ et al., 2013). Thus, the fabrication of hybrid constructs from fibrin and spider silk represents a promising approach for enhancing the biomechanical stability of fibrin-based vascular grafts.

In this work, we developed a novel coiling technique in order to integrate a supportive spider-silk network into the abluminal surface of highly compacted tubular fibrin matrices to generate bioartificial fibrin-based vascular grafts that provide sufficient structural resilience to withstand physiological and supraphysiological mechanical stress, resemble the elastic properties of native arteries and provide a sufficient suture retention strength for surgical anastomoses. Biomechanical behavior of the hybrid grafts was characterized by 2-dimensional and 3-dimensional mechanical testing and compared to spider silk free fibrin grafts.

2. Methods

2.1. Generation of the hybrid vascular graft

Hybrid grafts consisting of a spider silk reinforced highly compacted fibrin matrix were generated using a three step approach (Fig. 1).

In the first step, a tubular fibrin-based matrix was fabricated using a custom-built casting mold constructed by the Department of Medical Device Construction, Hannover Medical School (Fig. 2A). The casting mold consisting of polyether ether ketone (PEEK) facilitated molding of a tubular fibrin-based matrix with an outer diameter of 8 mm and a total length of 12 cm. A central placeholder with an outer diameter of 2.5 mm was inserted to create the lumen of the tubular matrix. The total molding volume was 5.44 cm^3.

For the molding of the tubular fibrin-based matrix, fibrinogen was isolated by cryoprecipitation from human plasma obtained from healthy donors at the blood donation service at Hannover Medical School after informed consent (Institute of Transfusion Medicine, Hannover, Medical School) as previously described (Lau, 2017). Fibrinogen obtained from 100 fresh frozen plasma donations was pooled. The fibrinogen-solution was supplemented with 100 µl x ml^{-1} Medium 199 10x (Sigma Aldrich, Steinheim, Germany), 1 µl x ml^{-1} Aprotinin (Bayer, Leverkusen, Germany) as well as titrated with 1N NaOH for pH-adaption resulting in a final fibrinogen concentration of 34.5 mg x ml^{-1}. By adding the activating solution containing 0.5 U x $µl^{-1}$ Thrombin and 0.06 U x $µl^{-1}$ Factor XIII (CSL Behring, Marburg, Germany) replenished in 40 mM $CaCl_2$ solution (CSL Behring, Marburg, Germany) the polymerization process was initiated. Immediately after mixing, the casting solution was filled into the tubular mold followed by a 15 min incubation period at room temperature for initial polymerization.

Afterwards, the tubular fibrin structure on the central placeholder was extracted from the mold and mounted on the specifically designed coiling machine for abluminal wrapping with spider silk (Fig. 2B). The silk was coiled directly as it was harvested from the silk gland of *Trichonephila edulis* that is kept and bred for scientific purposes at the Kerstin Reimer's Laboratory (Department of Plastic, Esthetic, Hand and Reconstructive Surgery at Hannover Medical School) according to a previously established techniques (Liebsch et al., 2020). Briefly, the spiders were extracted from their web and gently fixated on polystyrene blocks so that the silk could be drawn from the major ampullate glands. Although the female spider produces several varying silks, the dragline silk originating from the major ampullate of the silk gland was used for this application due to the biological and mechanical characteristics of *Trichonephila* dragline silk.

The automated coiling device consists of two step-motors: the first motor (10 in Fig. 2) drives a sled (9 in Fig. 2) for translational shift in the longitudinal direction, while the second motor (7 in Fig. 2) is mounted on the sled and facilitates rotation of the fibrin graft. The central placeholder holding the fibrin construct can be mounted onto the coiling machine using a drill chuck (8 in Fig. 2). Spider silk is guided using a guidance arm attached to the coiling machine (6 in Fig. 2). With that, it allows for the small caliber tubes to be coiled with spider silk by simultaneous translational shifting in the longitudinal direction and rotation around the central axis of the mounted fibrin matrix. While the rotation direction and speed remained constant at 88 rpm, the direction of the longitudinal shift was reversed after a distance of 5 cm resulting in a forth and back movement of the graft. The coiling machine was operated via a touchpad (11 in Fig. 2) and the corresponding operating sequence described above was programmed based on a C++ code and automated via an Arduino mega 2560 microcontroller board (Arduino SA, Lugano, Switzerland). This way, a reverse, intersecting coiling pattern of the spider silk network encapsulating the fibrin-graft was developed (Step 2 in Fig. 1). The angle of the fiber with respect to the axis of the silking device was kept at approximately 90° using the guidance arm that was placed closely to the fibrin segment (6 in Fig. 2). The average distance between consecutive silk threads was 3.3 mm ±

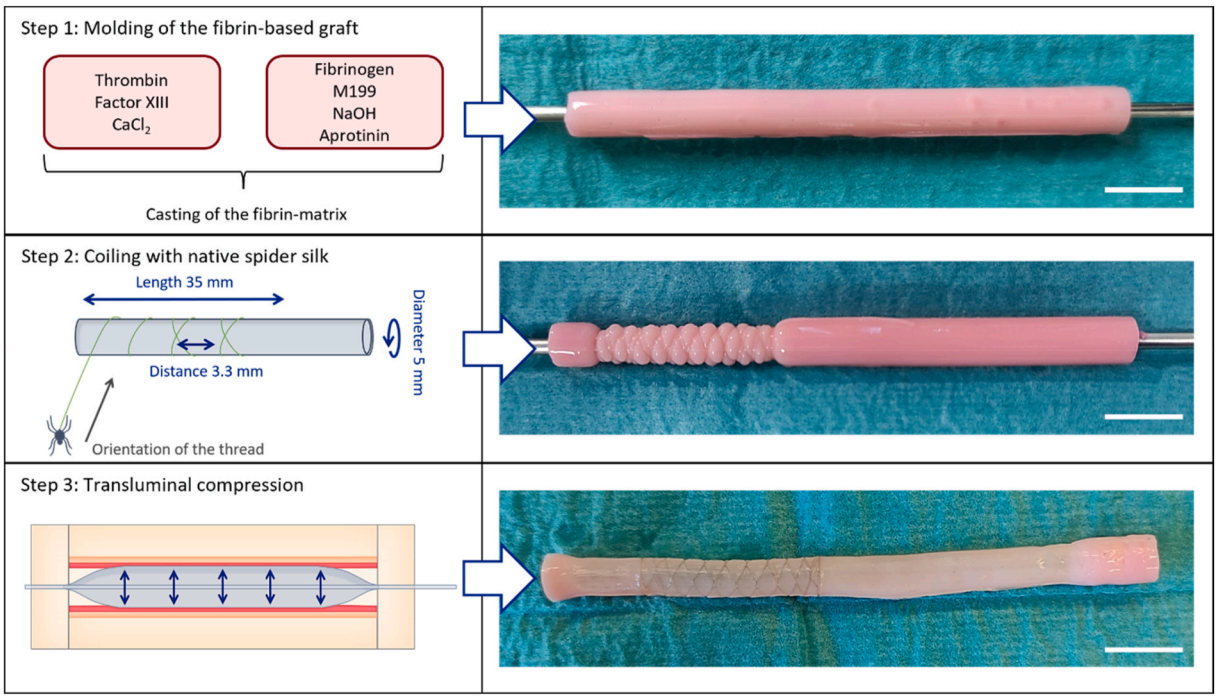

Fig. 1. Schematic flow chart of the generation of spider silk reinforced fibrin grafts. Step 1: Casting of the fibrin-matrix around a central metal placeholder in a custom built tubular mold. Step 2: Harvesting and coiling of native spider silk around the unprocessed fibrin-based graft with a custom built coiling machine. Here, grafts were simultaneously rotated and shifted along the longitudinal axis in a forth and back motion to generate a intersecting spider silk coiling pattern. Step 3: Transluminal compression of the hybrid fibrin graft with an intraluminal angioplasty dilatation balloon. M199 = Medium 199, Scale bar = 1 cm.

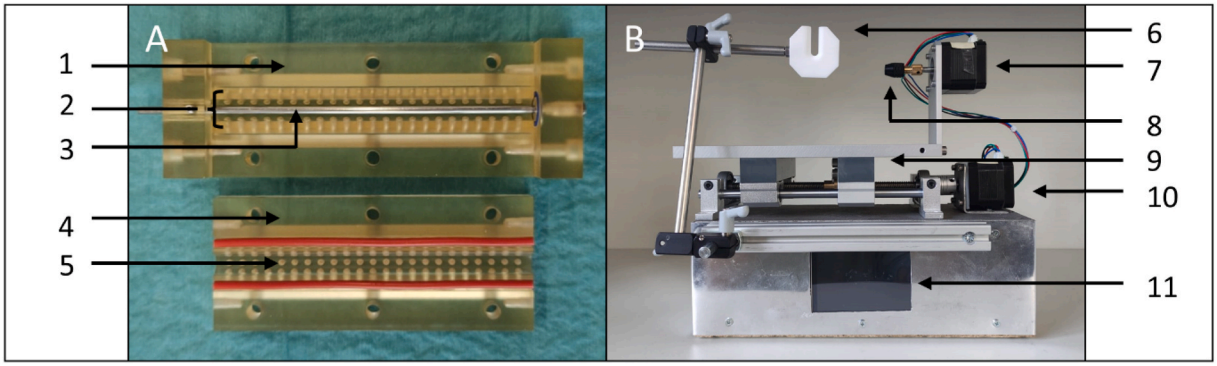

Fig. 2. Graft fabrication devices. A: Casting and compression mold; 1: main half of the vascular mold, 2: tubular cast diameter: 8 mm, 3: hollow metal placeholder (diameter 2.5 mm), 4: top half of the vascular mold, 5: drainage holes; B: Coiling machine; 6: guidance arm, 7: rotational step motor, 8: drill chuck, 9: sled, 10: translational step motor, 11: Touchpad.

0.3 mm. The vessel was coiled with spider silk for a total of 6 min generating a 3.5 cm long coiled segment depositing on average 42 layers of silk for each direction onto the graft. Total spider silk length per segment was 13.27 m corresponding to a harvesting speed of 2.21 m/min. The remaining part of the vascular graft was not coiled with silk and served as the control group.

After the coiling process, the fibrin grafts with or without spider silk sheathing were placed back onto the luminal placeholder in the same mold used for casting the graft. Subsequently, an 8 mm × 100 mm angioplasty dilatation catheter (POWERFLEX™ PRO 6F, 8.00 mm × 100 mm; 80 cm, Cordis Corporation, Miami, USA) was inserted into the hollow placeholder, which was then carefully removed setting the balloon free inside the tubular matrix. The balloon was then filled with purified water using an inflation device (Basix Compak™, Merit Medical, South Jordan, USA) to carefully increase the pressure until a maximum of 4 bar was reached. This pressure was kept constant during a 60 min compression period. During this transluminal compression, the fibrin matrix was compressed and excess fluid was drained through the drainage holes of the casting and compression mold (5 in Fig. 2). Afterwards, the angioplasty balloon was deflated and the graft was gently removed from the collapsed balloon and the casting mold (Step 3 in Fig. 1). All grafts were stored in phosphate buffered saline (PBS) containing 100 U x ml^{-1} Aprotinin and 1 % Penicillin/Streptomycin at 4 °C.

2.2. Biomechanical characterization

Biomechanical properties of spider silk reinforced fibrin grafts were characterized by both, 2-dimensional and 3-dimensional mechanical testing. For 2-dimensional testing uniaxial tests in form of tensile strength, compression pressure as well as suture retention strength analysis were performed. In 3-dimensional testing maximum burst pressure and compliance of the grafts were evaluated. A special focus was set on one hand on the biomechanical and elastic factors relevant to mimic the physiological behavior of native blood vessels in the fibrin-

based substitutes. On the other hand, biomechanical resilience with respect to surgical handling was investigated *in vitro*. Group size was n = 5 for each group in every test.

To determine the macroscopic dimensions of the grafts, a 5 mm long cross section of each control and hybrid graft was used to measure the mean inner and outer diameter as well as the wall thickness. Measurement was performed using a digital microscopic camera (Shen Zhen Technology Co. Ltd., Guangdong, China).

Uniaxial tensile strength was tested using 5 mm long segments of each vessel by placing them as loops onto two hooked metal rods (Fig. 4A) that were fixated in a linear mechanical testing machine (Zwick Roell, Ulm, Germany). The specimen were pulled apart continuously at 20 mm x min^{-1} until tearing of the loop. Applied force as well as dilatation length until structural failure were measured.

Moreover, the secant modulus of elasticity (E_s) was calculated using the following formula:

$$E_s = \frac{F_{max}}{\Delta\varepsilon}$$

with F_{max} = maximum force and $\Delta\varepsilon$ = elongation at F_{max}.

Compression pressure was measured using 3 cm long specimens of both, the spider silk reinforced hybrid graft and the control graft. For this, the specimen was placed in the mechanical testing machine (Zwick Roell, Ulm, Germany) that was now used to continuously compress the graft with a speed of 10 mm x min^{-1} until a maximum of 30 % deformation was reached (Fig. 5A). The compression pressure F_{max} (N) needed to achieve this deformation was measured. Three repeats of this testing process were performed for each specimen and mean compression pressure for each segment was calculated and used for statistical analysis.

Additionally, the maximum suture retention strength was investigated by placing a 5 mm segment into the linear uniaxial testing machine and inserting a single stitch with a 6-0 Prolene suture (Ethicon, Puerto Rico, USA). Since anastomoses of small-diameter vessels require placing the suture close to the graft edge to avoid narrowing of the anastomosis sites, the suture was placed with a 1 mm distance from the free edge of the sample (Fig. 5C). With the segment on one side and the end of the thread on the other side, the suture was pulled continuously until rupture of the specimen at the site of the stitch. The maximum force at tearing of the segment was measured.

In the three-dimensional testing, the compliance was measured as recently described (Helms et al., 2021b). Briefly, 2 cm long segments of the grafts were placed in a custom-built perfusion test chamber and filled with PBS. Each end was fixated onto an adaptor using a 2-0 ligature (Ethicon, Diegem, Belgium, Fig. 6B). To create a sinusoidal pressure curve with a pulse frequency of 60 bpm, a pulsatile peristaltic pump (Ismatec, Steinheim, Germany) was installed. A digital pressure sensor (Comark ltd., Norwich, England) was used for continuous measurement and the pressure curve was visualized using a clinical pressure monitoring system (Datex Ohmeda S 5, Helsinki, Finland). In order to control the mean pressure, a manual pressure syringe (SIS Medical AG, Frauenfeld, Switzerland) was integrated into the system. While adapting of the pressure amplitude to 40 mmHg for each sample, the intraluminal pressure acting on the probes could be increased until the desired pressure range of 120 over 80 mmHg was reached. During the testing process, the specimen was continuously recorded using a digital microscopic camera (Shen Zhen Technology Co. Ltd., Guangdong, China) to measure the maximum and minimum outer diameter during the pulsatile stimulation. Afterwards, the compliance (C) at a mean pressure of 100 mmHg was calculated using the following formula described by Fernandez-Colino et al. (Fernández-Colino et al., 2019):

$$C = \frac{((D_{max} - D_{min})/D_{min}) \times 10^4}{P_{max} - P_{min}}$$

with D_{max} = maximum diameter, D_{min} = minimum diameter, P_{max} = maximum pressure and P_{min} = minimum diameter.

In addition, the stiffness index (β) could be calculated using the following formula (Soletti et al., 2010):

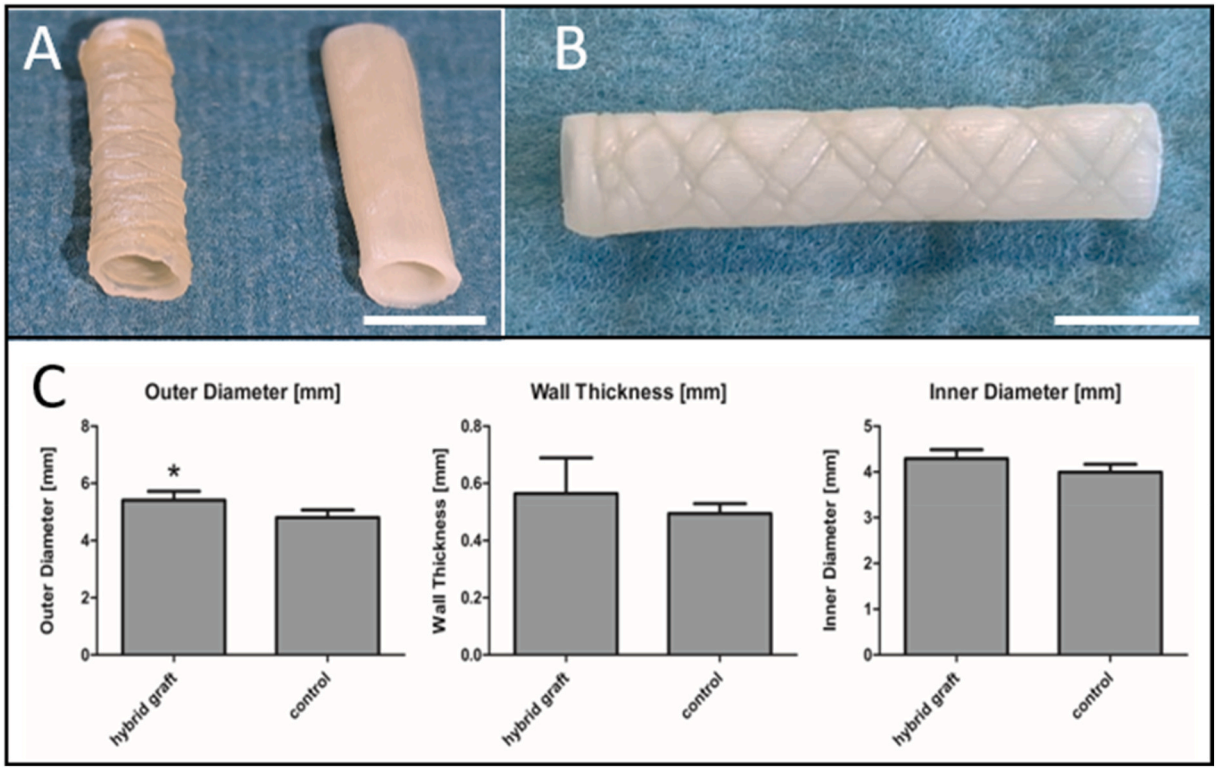

Fig. 3. Graft morphology. A: comparative cross section, left: spider silk reinforced graft, right: control graft; B: abluminal top view of a spider silk reinforced fibrin graft C: Quantification of vessel dimensions. Scale Bar = 5 mm.

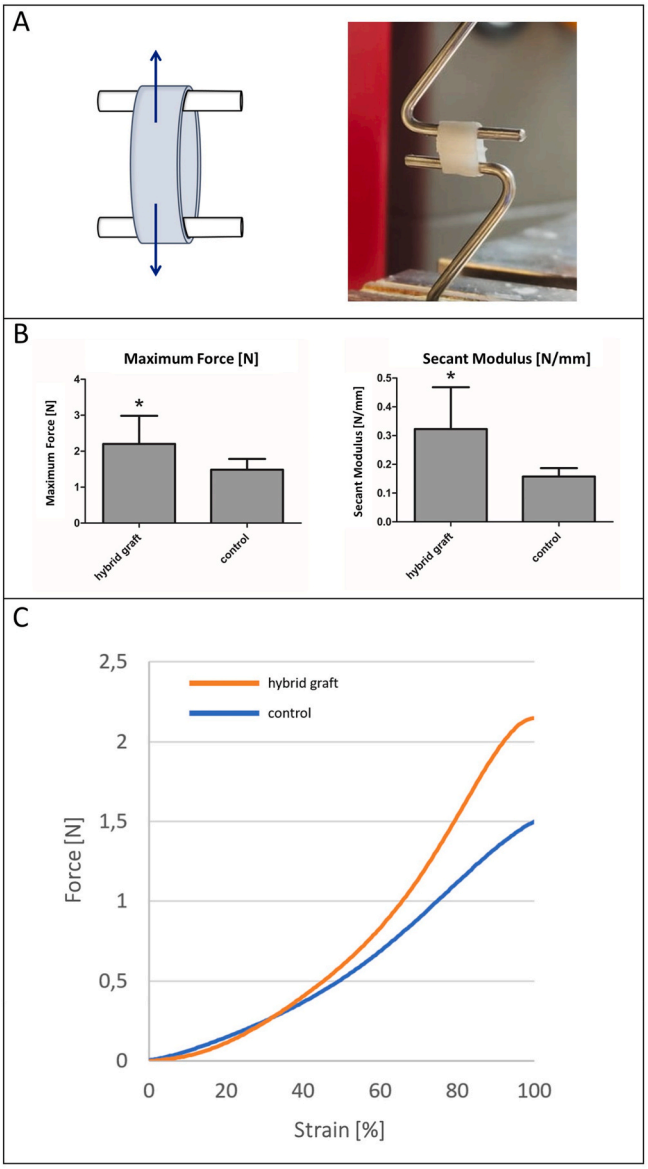

Fig. 4. Uniaxial tensile test. A: loop testing method. A 5 mm segment of the graft was placed between two metal hooks, which were pulled in opposite directions. The maximum force before structural failure was measured. B: absolute tensile strength and secant elastic modulus, C: stress/strain analysis of the hybrid grafts (red) and pure fibrin controls (blue). 6th order polynomial regression was performed for each group.

$$\beta = \frac{\ln\left(P_{max}/P_{min}\right)}{\left(D_{max} - D_{min}\right)/D_{min}}$$

with P_{max} = maximum pressure, P_{min} = minimum pressure, D_{max} = maximum diameter and D_{min} = minimum diameter.

Furthermore, the burst pressure was measured as previously described (Helms et al., 2021b) using the same testing system as for the compliance test set up. Briefly, one end of the segment was occluded and the segment was then filled with PBS with a continuous flow rate of 10 ml/min using a custom-built application system (Department of Medical Device Construction, Hannover Medical School) until burst. During the testing process, the maximum pressure directly before burst of the specimen was recorded using the digital pressure sensor (Codan PVB Critical Care GmbH, Forstinning, Germany). The outer diameter at burst was again recorded. The wall thickness at burst was calculated using the diameter at burst as well as the inner and outer diameter of the vascular graft. Subsequently, the absolute wall tension (T) was calculated as follows:

$$T = P \times r$$

with P = pressure at burst and r = radius at burst.

On the basis of the burst pressure, outer diameter and wall thickness at burst, the maximum wall stress (σ) could be determined:

$$\sigma = P \times \frac{r}{u}$$

with P = pressure at burst, r = radius at burst and u = wall thickness at burst.

2.3. Scanning electron microscopic analysis

For scanning electron microscopic analysis of the grafts, 3–5 mm long segments were cut from the fabricated vessels and fixated in a solution containing 1,5 % Paraformaldehyde, 1,5 % Glutaraldehyde and 150 mM HEPES buffer at pH 7,35 for at least 24 h before preparation for scanning electron microscopy (SEM) using Zeiss Crossbeam 540-47-80 microscope (Carl Zeiss, Oberkochen Germany) (Institute of Functional and Applied Anatomy, Hannover Medical School). Samples were analyzed in several magnifications varying from 50X – 10.000X magnification obtaining cross sectional as well as luminal and abluminal plane views.

2.4. Evaluation of the endothelialization capacity

To investigate a potential negative impact of spider silk coiling around the fibrin grafts on the luminal fibrin surface integrity and thus, on the formation of a luminal endothelial monolayer, the *in vitro* endothelialization capacity of the spider silk reinforced grafts was assessed. To test luminal endothelial cell attachment, three 3 cm long samples of each group were excised from the vessel and seeded with red fluorescent protein expressing human umbilical vein endothelial cells (RFP-HUVEC, Pelo Biotech, Planegg, Germany) as described previously (Helms et al., 2021a). Briefly, the segments were fixed onto Luer lock®-adaptors using a 2-0 silk ligature (Ethicon, Diegem, Belgium) on each end. Each segment was filled with 3 x 10^6 RFP-HUVECs suspended in endothelial growth medium 2 (EGM2, Lonza, Basel, Switzerland). Both ends of the adaptors were tightly closed and the segments were gradually rotated over a course of 90 min at 37 °C and 5 % CO_2 in order to allow circular cell attachment. After this, the adaptors were opened and the specimen were incubated in EGM2 for another 24 h at 37 °C and 5 % CO_2. Thereafter, the cell attachment to the luminal surface of the samples was visualized using fluorescent microscopy (Nikon Eclipse TE300, Düsseldorf, Germany). Cell viability was assessed by immunofluorescence staining. Therefore, cellularized segments were incubated in Dulbecco's modified eagle medium (DMEM) supplemented with 0.5 µmol x L^{-1} Calcein (Life Technologies, Darmstadt, Germany) for 45 min prior to immediate fluorescence microscopic imaging.

2.5. Statistics

For comparison of the two matched groups, one-tailed Wilcoxon matched-pairs signed-rank test was performed. Values are given as mean ± standard deviation. Results were considered significant at $p < 0.05$ and marked with an asterisk (*) in the corresponding graphs.

3. Results

3.1. Macroscopic morphology

Macroscopically, the coiling pattern appeared consistent and intact creating an evenly distributed framework covering the abluminal

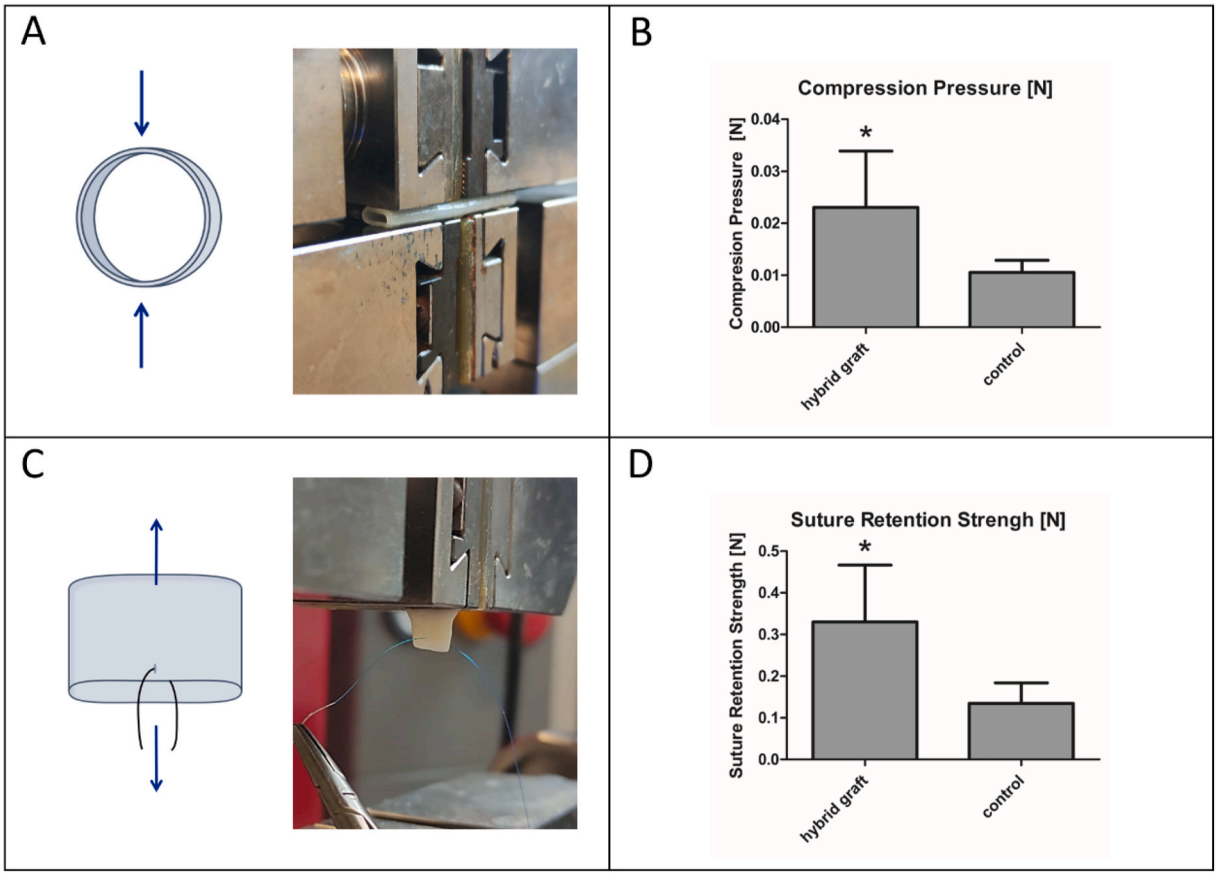

Fig. 5. Compression and suture retention. A: compression test method. 3 cm long segments are externally compressed, maximum resistance force exhibited by the graft at 30 % compression was measured B: compression test results, C: suture retention test method. A 6-0 Prolene suture was paced at the free edge of the probe and pulled down. Maximum suture retention strength was measured. D: suture retention strength results.

surface of the fibrin-matrix as shown in Fig. 3A and B. Upon qualitative assessment, structural connection between the fibrin matrix and the spider silk network appeared to be strong with no signs of unintended layer separation or uncoiling after transluminal compression.

For quantitative assessment of the impact of the spider silk framework on the morphology of the fibrin-vessels, graft dimensions regarding wall thickness and diameters were measured. Only minimal changes were observed concerning the wall thickness with an average of 0.56 mm ± 0.11 mm in the spider silk coiled grafts compared to a mean wall thickness of 0.50 mm ± 0.03 mm in the control group. Similarly, there was no significant change in the inner diameter after coiling whereas the outer diameter in the coiled vessels was slightly increased compared to the solely fibrin-based grafts. (Fig. 3C).

3.2. Biomechanical characterization

The biomechanical properties of the hybrid grafts were investigated using two-dimensional tests as well as three-dimensional compliance and burst pressure measuring techniques.

Here, the group of spider silk-reinforced grafts showed a significant increase in the absolute tensile strength compared to the control grafts with 2.2 N ± 0.7 N in the spider silk-coiled grafts and 1.49 N ± 0.27 N without spider silk reinforcement. Accordingly, a significantly higher secant modulus could be detected (Fig. 4 B). The stress/strain diagram (Fig. 4C) shows a sigmoidal curve form for both, the hybrid grafts and the control samples. With a similar stress/strain behavior at low strains, the curves divert at approximately 30 % of maximum strain with the hybrid grafts surpassing the control samples.

Furthermore, a higher resistance against external compression of the bioartificial hybrid vessels compared to the control group was observed (Fig. 5B).

Likewise, adding a supplementary spider silk framework to the fibrin-based vascular grafts resulted in a higher suture retention strength indicated by a significant 2.45-fold increase in stability until rupture of the segment (Fig. 5D).

During the three-dimensional testing, the behavior of the bioartificial vessels in respect of the compliance as well as stiffness properties were evaluated by measuring the minimum and maximum diameter of the vascular graft at a mean pressure of 100 mmHg and a pressure amplitude of 40 mmHg (Fig. 6). Although not reaching statistical significance, a slight decrease in the compliance of the fibrin-based grafts after coiling with the dragline silk was noted in conformity with an 1.39-fold increase of the stiffness index in these hybrid grafts (Fig. 6C) suggesting a lowered compliance due to the stiffening character of the silk framework.

Additionally, a distinct increase in the maximum burst pressure could be seen with a mean pressure of 362 ± 74 mmHg in the coiled samples compared to 213 ± 14 mmHg ($p < 0.05$) in samples without spider silk. The diameter directly before burst was approximately the same in both groups (Fig. 6C). Consistent to the observed increase in burst pressure, spider silk reinforced grafts also showed a significantly higher maximum wall tension. Opposed to that, no significant increase of the wall stress could be detected after coiling.

3.3. Scanning electron microscopic analysis

To investigate the ultrastructure of the spider silk reinforced fibrin grafts, scanning electron microscopy was performed of the luminal and

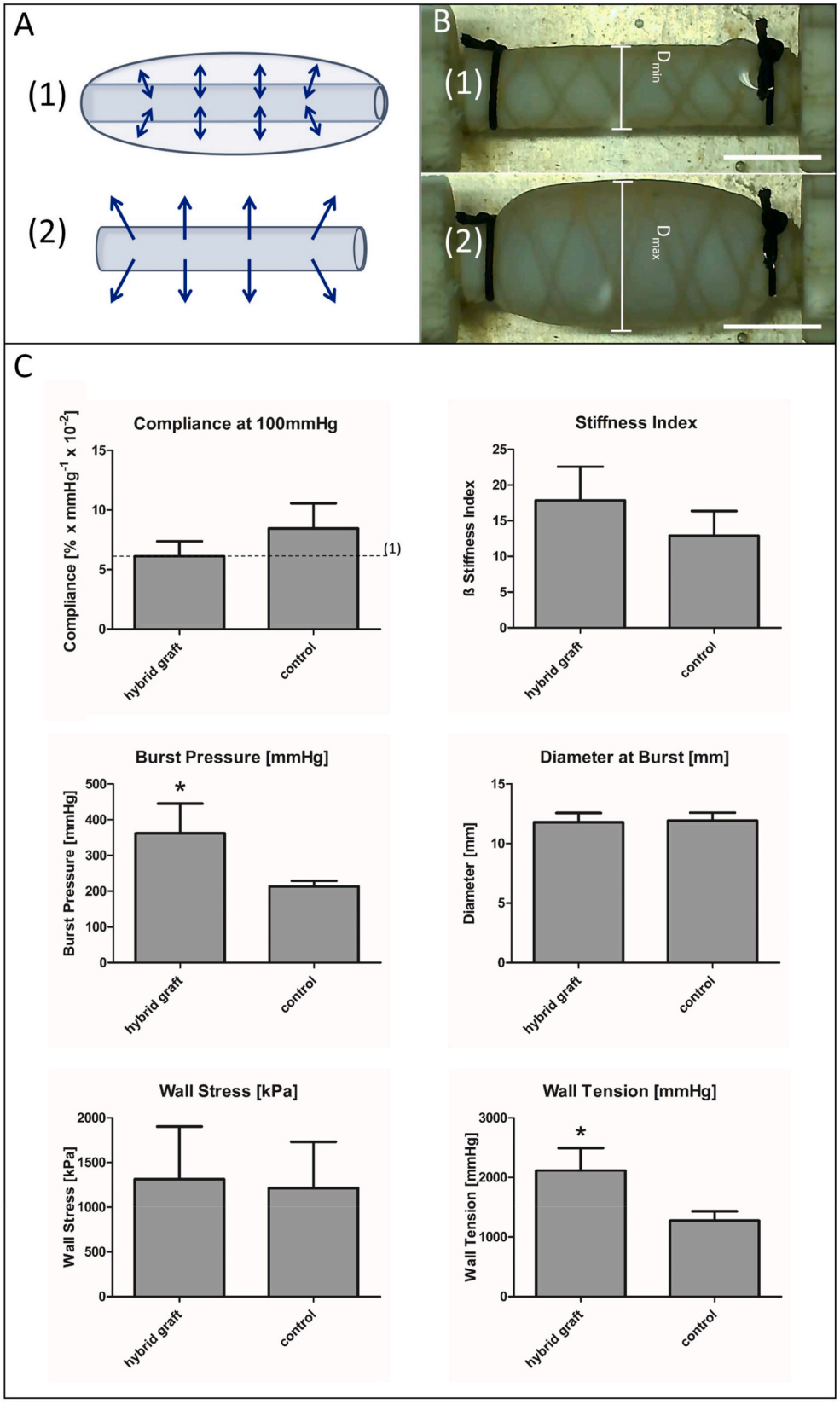

Fig. 6. Three-dimensional mechanical characterization. A: schematic representation of the compliance testing method (Dicker et al., 2018) and burst pressure test (Formichi et al., 1988). B: top view of a spider silk reinforced fibrin graft after insertion into the test device at minimum diameter (Dicker et al., 2018) and maximum diameter (Formichi et al., 1988) during compliance testing at 120/80 mmHg. C: Compliance- and burst test results. The compliance at 100 mmHg was compared to physiological values of natural human umbilical arteries (dotted line 1), obtained from Gui et al. (Gui et al., 2009). Scale bar = 5 mm.

abluminal surface and of cross-sections for both, the hybrid vascular grafts and the control samples (Fig. 7). In each group, a homogenous and dense luminal structure of the fibrin-network was seen as a result of the efficient compaction of the matrix (Fig. 7A). At a magnification of 200X, the exclusively abluminal positioning of the silk-framework was confirmed (Fig. 7B). While the abluminal surface inevitably becomes uneven due to the integrated spider silk framework, the luminal wall appears to stay entirely smooth after coiling (Fig. 7B). Scanning electron microscopy revealed that the spider silk network was not tightly fused with the fibrin matrix but rather forms a separate network on the abluminal surface of the grafts. This phenomenon was observed with high consistency in different views and preparations (Fig. 7B, C).

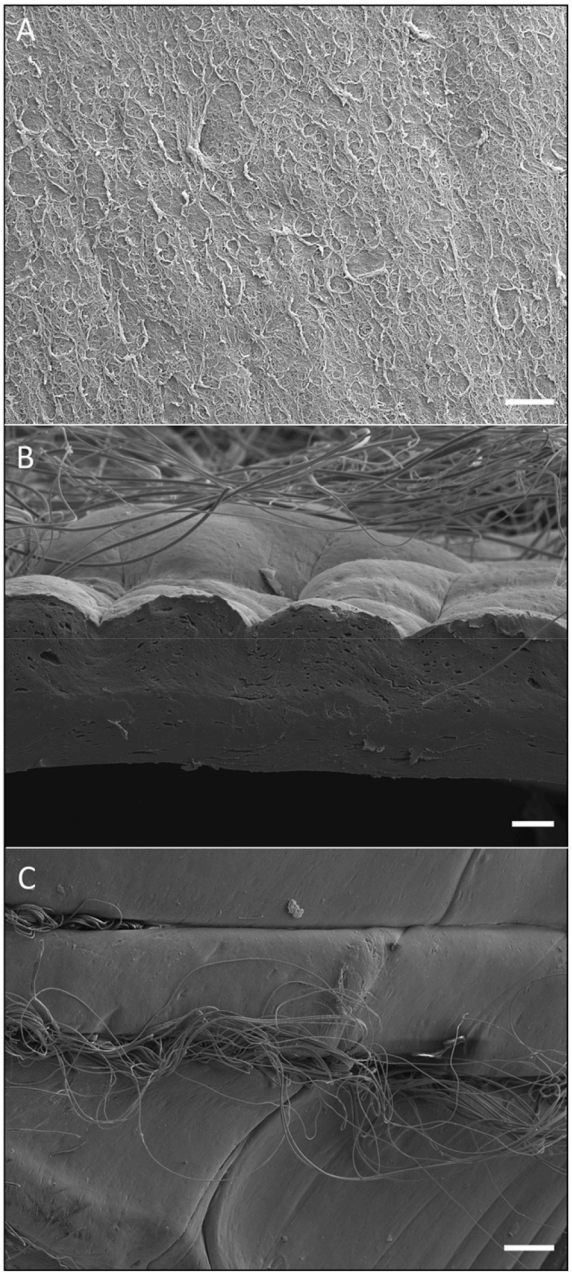

Fig. 7. Scanning electron microscopy of spider silk reinforced grafts. A: Top view of the luminal surface, magnification: 1000X, scale bar = 10 μm; B: cross section view through the fibrin graft. The abluminal surface is shown on the top and the luminal surface on the bottom half, magnification: 200X, scale bar = 40 μm; C: Top view of the abluminal surface, magnification: 100X, scale bar = 100 μm.

3.4. Endothelialization capacity

In order to qualitatively evaluate the impact of integrating spider silk into fibrin-based vascular grafts on the capacity for endothelialization and cell attachment, samples of both groups were seeded with RFP-HUVECs and analyzed by fluorescent microscopy. Here, while considering manual mechanical damage during sample preparation, a confluent and homogeneous endothelial cell layer could be observed in the spider silk reinforced vessels. On qualitative assessment, no differences concerning the endothelialization capacity between the two groups were found (Supplementary Fig. S1). Calcein staining revealed high cell viability after 24h of incubation (Fig. 8).

4. Conclusions

In this study, we generated a spider silk reinforced fibrin-based vascular graft using a novel coiling technique. Thorough biomechanical characterization of the hybrid grafts was performed as a proof of concept for this newly developed prosthesis. The new findings can be summarized as follows: 1) The coiling and compression technique is suitable for the generation of hybrid vascular grafts consisting of a highly compacted fibrin matrix and supportive spider silk network. 2) Spider silk reinforced grafts provide superior biomechanical stability compared to solely compacted fibrin based vessels with respect to burst pressure, tensile strength, and resistance to external compression. 3) Addition of spider silk reduces compliance of fibrin grafts resulting in a more physiological elastic behavior compared to native vessels. 4) The hybrid prostheses allow confluent endothelialization *in vitro*.

4.1. Coiling and compression technique

For the generation of mechanically stable fibrin-based vascular grafts, two techniques that have previously been proven to be effective for enhancing the biomechanical stability of fibrin structures were combined: First, the fibrin tube was surrounded by a supporting spider silk network and second, the fibrin matrix was compacted by transluminal compression.

For this, we established a novel coiling technique for the application of spider silk onto fibrin tubes based on a reverse intersecting coiling pattern. This process was automated by a custom built coiling device and resulted in a reliable and homogenous coiling pattern of the spider silk network (Fig. 3B). Addition of spider silk in fibrin-based constructs was first performed for the generation of fibrin-based cardiac patches (Bobylev et al., 2021). In that work, spider silk derived from the cocoons of *Trichonephila edulis* spiders was integrated in plane circular fibrin matrices that served as patches for cardiac applications. In that work, integration of spider silk enhanced biomechanical stability of the patches and especially improved suture retention strength which allowed surgical implantation into the right ventricular outflow graft in sheep. Similar observations were made in the spider silk enhanced fibrin grafts which also show superior biomechanical stability and suture retention strength *in vitro*. While for the patches, spider silk cocoons could be used directly and no sophisticated weaving technique was required since the plane patches have less complex morphology compared to the vascular grafts, a coiling technique using the dragline silk was necessary for the tubular fibrin prosthesis. The automated weaving technique facilitated generation of a homogeneous spider silk framework on the abluminal surface of the fibrin-based grafts. Since coiling was performed directly after initial polymerization of the fibrin matrix, the subsequent transluminal compression by the angioplasty balloon pressed the fibrin matrix firmly into the spider silk network resulting in a tight connection (Fig. 3A). Contrary to that, scanning electron microscopic analysis showed no fusion of the spider silk fibers into the fibrin matrix, but rather abluminal spider silk bundles resting on the fibrin tubes (Fig. 8B). Nonetheless, no signs of uncoiling or spider silk network dissociation were detected upon macroscopic qualitative

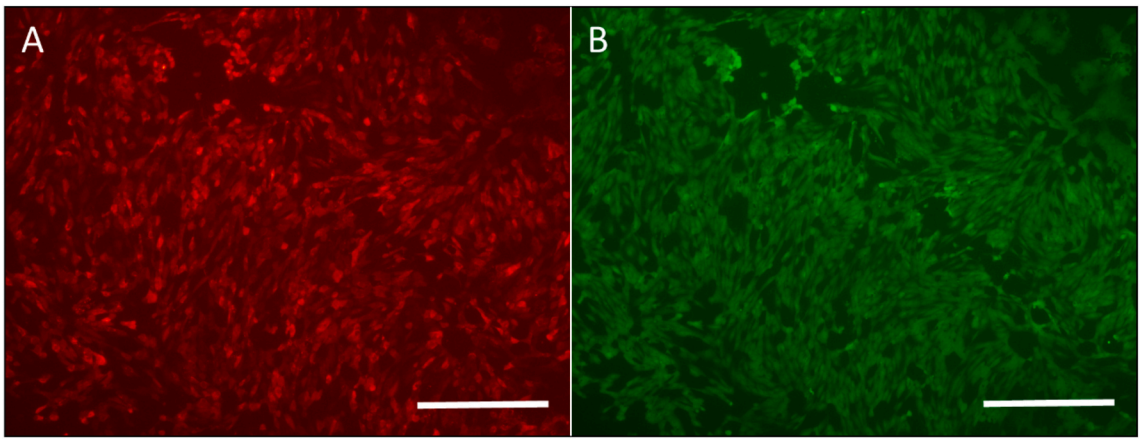

Fig. 8. Endothelialization capacity. Red fluorescent protein expressing human umbilical vein endothelial cells were seeded onto the luminal surface of spider silk reinforced fibrin based vascular grafts and incubated for 24 h. A: view of the luminal surface, endothelial cells are marked in red by red fluorescent protein, B: Calcein cell viability test of the same view shown in A. Viable cells are marked green by Calcein staining. Scale bar = 500 μm.

assessment.

A completely different approach for using spider silk to generate bioartificial vascular prostheses was established by Dastagir et al. (2020): They used a spider silk network as a base structure for extracellular matrix construction by myoblasts *in vitro*. For that, spider silk was woven by hand on 2-dimensional frames and later sutured to create a tubular structure that was seeded with myoblasts and cultured in a dynamic bioreactor. While these bioartificial vessels provided excellent stability, the production and culture period with three weeks of mechanical stimulation in a bioreactor system was comparably long. Moreover, murine myoblasts were used for extracellular matrix production, which is problematic with respect to storage and translational applications in humans. Compared to that, the production time of the spider silk reinforced fibrin grafts was only approximately 2 h. Since we use a cell-free approach, no bioreactor cultivation was necessary and grafts can be stored in PBS at 4 °C, which potentially provides *off the shelf* availability. The effect of long-term storage of fibrin-based vascular grafts has been investigated in a previous work, where fibrin grafts were found to be generally suitable for *off the shelf* application (Aper et al., 2018). Nonetheless, the results of Dastagir et al. showed that the application of spider silk in vascular tissue engineering is suitable and provides not only mechanical strength, but also functions as a cell carrier for cell types relevant for bioartificial vessel generation. Likewise, the addition of spider silk in fibrin-based bioartificial grafts did not impair *in vitro* endothelialization capacity in our work (Fig. 8). In this study pooled fibrinogen of numerous donors was used. While this technique was highly useful to avoid variations in fibrinogen quality and concentration, the use of fibrinogen of only one donor or the patients themselves is undoubtedly a desirable goal with respect to translational approaches.

4.2. Biomechanical properties

Spider silk reinforcement resulted in a statistically significant increase of the biomechanical stability as indicated by both, 2-dimensional tensile strength and burst pressure. In the latter, a mean burst pressure of 362 ± 74 mmHg was achieved which is well above the blood pressure peaks in the human body that can be reasonably expected. Considering the maximum tensile force, larger variances were observed in the spider silk reinforced group which is most likely due to variances in the quality of the spider silk as a biological material. Compared to the biomechanical stability achieved by transluminal balloon compression alone (Helms et al., 2021b) or compaction of the fibrin matrix by centrifugation (Aper et al., 2016), spider silk reinforcement facilitates additional strengthening of the graft wall resulting in higher burst pressure than what can be achieved by fibrin compaction alone. As shown in the 3-dimensional measurements of wall stress and tension, spider silk reinforced grafts resisted a significantly higher wall tension, while wall stress at burst was similar in both groups. Thus, the increase in burst pressure is most likely mediated by regulation of the wall stress by spider silk reinforcement. While this mechanical stability is distinctively higher compared to previously reported fibrin-based vessels (Gui et al., 2014; Isenberg et al., 2006; Helms et al., 2022), burst pressure of the spider silk reinforced hybrid grafts was still distinctively lower compared to native arteries, which regularly withstand pressures of well over 800 mmHg (Böer et al., 2015). However, spider silk enhancement increases the desired safety margin relevant to avoid graft failure due to unexpected pressure peaks or external forces.

In this work, the fibrin-based vessels were tested for the first time for their resistance to external pressure. Spider silk reinforcement resulted in a twofold increase in the compression resistance force (Fig. 5). In order to prevent collapse under external pressure, this radial resistance is essential if the prostheses are to be used in locations subject to high mechanical stress, such as near a joint or on the distal extremities.

Similar observations were made with respect to suture retention strength. Here, spider silk reinforcement led to a statistically significant increase of suture retention strength compared to the solely compacted control group. These observations are consistent with previous findings by Bobylev et al. on the influence of spider silk reinforcement in fibrin-based cardiac patches (Bobylev et al., 2021). In that previous work, patches supplemented with a spider silk cocoon also showed superior suture retention strength and favorable results in *in vitro* sewing tests compared to pure fibrin patches. However, commonly used native graft vessels still provide a significantly higher suture retentions strength than the bioartificial constructs generated here. Likewise, the maximum burst pressure of native vessels commonly used as bypass material is still distinctively higher than what can be achieved with the hybrid grafts (Konig et al., 2009).

In addition to maximal strength measurements, the elastic properties of the grafts were compared. Here, a significantly higher secant modulus as well as a slight increase in stiffness was observed in the spider silk reinforced group. This correlated with a decrease in compliance at a physiological pressure amplitude of 120 over 80 mmHg. Interestingly, the stress strain behavior of the spider silk reinforced grafts and the solely compacted controls was similar up to 30 % of maximum strain. With higher strain, the curves diverted with distinctively higher stresses acting on the spider silk reinforced grafts. This phenomenon can potentially be attributed to the morphology of the abluminal spider silk fibers observed in scanning electron microscopy (Fig. 7B, C). Despite macroscopically dense winding, the spider silk bundles appeared

twisted and with a certain distance to the fibrin surface by electron microscopy. Consequently, it seems likely that the stress strain behavior at low strain is primarily determined by the compacted fibrin matrix and only at higher strain by the subsequently tensed spider silk fibers. This phenomenon results in higher compliance at lower pressures and vice versa. The inverse correlation of compliance and pressure is also seen in native arteries (Tai et al., 2000) and thus, it may be considered a supporting factor in the effort to generate a bioartificial graft with the most biomimetic biomechanical behavior possible.

Concerning the three-dimensional compliance measurements, spider silk reinforced grafts showed elastic properties comparable to human umbilical arteries (Gui et al., 2009) and the great saphenous vein (Tai et al., 2000), while the human internal mammary artery was reported to have considerably higher compliance of approximately 11 % per 100 mmHg (Konig et al., 2009). Compared to that, currently available synthetic graft materials show only minimal to no compliance (Tai et al., 2000).

4.3. Spider silk as a supportive scaffold

In our approach, silk produced by female *Trichonephila edulis* was used as a supportive scaffold surrounding the fibrin-based grafts. While the silk products of arachnids, insects or worms such as *Bombyx mori* silkworms have been used as natural polymers for various medical applications for centuries, in recent years they were used with increasing interest in tissue engineering approaches as well (Zhang et al., 2021; Salehi et al., 2020). As in our approach, spider silk fibers are predominantly used to enhance the biomechanical stability of tissue engineered constructs due to its outstanding biomechanical strength. With an unique balance of strength, extensibility and stiffness at a minimal diameter, spider dragline silk outperforms most natural and synthetic fibers (Vollrath, 2000; Fu et al., 2009; Rising et al., 2005; Young et al., 2021; Blamires et al., 2023; Garrote et al., 2020). Additionally, spider silk has been shown to have adequate bio- and hemocompatibility as well as being degradable *in vivo* (Allmeling et al., 2008b; Kuhbier et al., 2017b). Likewise, no adverse effects of spider silk on the integrity of the fibrin matrix or on the endothelialization capacity were observed in our study. However, Koop et al. recently reported a granulomatous foreign body reaction against constructs consisting of fibrin and spider silk implanted into the spinal cord of rats (Koop et al., 2022). As Koop et al. discuss, this adverse immunological response may have been a phenomenon of the specific immunological environment of the central nervous system of rats. Thus, it should not generally preclude the application of spider silk in the peripheral vasculature. Considering the detailed knowledge of the composition of the silk, the comparable biomechanical behavior and the secure utilization of the silk, the dragline of *Trichonephila* spp. appears to be the most suitable spider silk to be used for this specific vascular tissue engineering approach.

4.4. Endothelialization capacity

While physiological biomechanical properties and elastic behavior are undoubtedly critical factors for bioartificial graft generation, bioengineered vascular grafts should allow for cellularization in order to generate biologically active vascular prostheses. For this, endothelialization capacity and endothelial cell viability was tested in the spider silk reinforced grafts. Here, a confluent endothelial cell layer and satisfactory cell viability were observed. Scanning electron microscopy revealed that spider silk fibers were positioned strictly abluminal and did not alter the luminal surface morphology of the fibrin matrix, which was smooth and homogenous (Fig. 7A). Thus, the endothelialization capacity of the fibrin matrix, which has been frequently reported previously (Helms et al., 2020, 2021a, 2021b; Isenberg et al., 2006), was not impaired by the spider silk reinforcement.

4.5. Conclusion and future perspective

In this *proof of concept* study, we developed a novel technique for the generation of spider silk reinforced fibrin based bioartificial vascular prosthesis with sufficient biomechanical stability to withstand physiological and supraphysiological mechanical stresses of the vascular system after implantation and facilitate suture retention during anastomoses. As a regenerative prosthesis with biomimetic elastic properties comparable to the physiological elastic behavior of native blood vessels and a high endothelialization capacity, spider silk reinforced fibrin grafts meet the demands for a true bioactive vascular prosthesis with potentially superior hemo- and biocompatibility. This potential will be investigated in first *in vivo* applications of the novel graft in the near future.

Funding

This study was supported by the German Heart Foundation/German Foundation of Heart Research, Grant No. F/52/21.

CRediT authorship contribution statement

Clara Glomb: Writing – review & editing, Writing – original draft, Visualization, Methodology, Investigation, Formal analysis, Data curation. **Mathias Wilhelmi:** Writing – review & editing, Supervision, Project administration, Funding acquisition. **Sarah Strauß:** Writing – review & editing, Resources, Funding acquisition. **Sarah Zippusch:** Writing – review & editing, Investigation. **Melanie Klingenberg:** Validation, Investigation. **Thomas Aper:** Supervision, Resources. **Peter M. Vogt:** Writing – review & editing, Supervision. **Arjang Ruhparwar:** Writing – review & editing, Supervision, Project administration. **Florian Helms:** Writing – review & editing, Writing – original draft, Supervision, Project administration, Investigation, Funding acquisition, Formal analysis, Data curation, Conceptualization.

Declaration of competing interest

The authors declare that they have no known competing financial interests or personal relationships that could have appeared to influence the work reported in this paper.

Data availability

Data will be made available on request.

Acknowledgements

We thank Emely Lange for her help with the spider silk harvest. Electron microscopy data was generated by use of the Research Core Unit Electron Microscopy, Hannover Medical School.

Appendix A. Supplementary data

Supplementary data to this article can be found online at https://doi.org/10.1016/j.jmbbm.2024.106433.

References

Allmeling, C., Jokuszies, A., Reimers, K., Kall, S., Choi, C.Y., Brandes, G., et al., 2008a. Spider silk fibres in artificial nerve constructs promote peripheral nerve regeneration. Cell Prolif. 41 (3), 408–420.

Allmeling, C., Jokuszies, A., Reimers, K., Kall, S., Choi, C.Y., Brandes, G., et al., 2008b. Spider silk fibres in artificial nerve constructs promote peripheral nerve regeneration. Cell Prolif. 41 (3), 408–420.

Aper, T., Wilhelmi, M., Gebhardt, C., Hoeffler, K., Benecke, N., Hilfiker, A., et al., 2016. Novel method for the generation of tissue-engineered vascular grafts based on a highly compacted fibrin matrix. Acta Biomater. 29, 21–32.

Aper, T., Wilhelmi, M., Boer, U., Lau, S., Benecke, N., Hilfiker, A., et al., 2018. Dehydration improves biomechanical strength of bioartificial vascular graft material and allows its long-term storage. Innov. Surg. Sci. 3 (3), 215–224.
Blamires, S., Lozano-Picazo, P., Bruno, A.L., Arnedo, M., Ruiz-León, Y., González-Nieto, D., et al., 2023. The Spider Silk Standardization Initiative (S3I): a powerful tool to harness biological variability and to systematize the characterization of major ampullate silk fibers spun by spiders from suburban Sydney, Australia. J. Mech. Behav. Biomed. Mater. 140, 105729.
Bobylev, D., Wilhelmi, M., Lau, S., Klingenberg, M., Mlinaric, M., Petená, E., et al., 2021. Pressure-compacted and spider silk-reinforced fibrin demonstrates sufficient biomechanical stability as cardiac patch in vitro. J. Biomater. Appl., 8853282211046800
Bobylev, D., Horke, A., Boethig, D., Hazekamp, M., Meyns, B., Rega, F., et al., 2022. 5-Year results from the prospective European multi-centre study on decellularized homografts for pulmonary valve replacement ESPOIR Trial and ESPOIR Registry data. Eur. J. Cardio. Thorac. Surg. 62 (5), ezac219.
Böer, U., Hurtado-Aguilar, L., Klingenberg, M., Lau, S., Jockenhoevel, S., Haverich, A., et al., 2015. Effect of intensified decellularization of equine carotid arteries on scaffold biomechanics and cytotoxicity. Ann. Biomed. Eng. 43 (11), 2630–2641.
Dastagir, K., Dastagir, N., Limbourg, A., Reimers, K., Strauß, S., Vogt, P.M., 2020. In vitro construction of artificial blood vessels using spider silk as a supporting matrix. J. Mech. Behav. Biomed. Mater. 101, 103436.
Dicker, D., Nguyen, G., Abate, D., Abate, K.H., Abay, S.M., Abbafati, C., et al., 2018. Global, regional, and national age-sex-specific mortality and life expectancy, 1950–2017: a systematic analysis for the Global Burden of Disease Study 2017. Lancet 392 (10159), 1684–1735.
Fernández-Colino, A., Wolf, F., Rütten, S., Schmitz-Rode, T., Rodríguez-Cabello, J.C., Jockenhoevel, S., et al., 2019. Small caliber compliant vascular grafts based on elastin-like recombinamers for in situ tissue engineering. Front. Bioeng. Biotechnol. 7, 340.
Formichi, M.J., Guidoin, R.G., Jausseran, J.M., Awad, J.A., Johnston, K.W., King, M.W., et al., 1988. Expanded PTFE prostheses as arterial substitutes in humans: late pathological findings in 73 excised grafts. Ann. Vasc. Surg. 2 (1), 14–27.
Fu, C., Shao, Z., Fritz, V., 2009. Animal silks: their structures, properties and artificial production. Chem. Commun. (43), 6515–6529.
Garrote, J., Ruiz, V., Troncoso, O.P., Torres, F.G., Arnedo, M., Elices, M., et al., 2020. Application of the Spider Silk Standardization Initiative (S3I) methodology to the characterization of major ampullate gland silk fibers spun by spiders from Pantanos de Villa wetlands (Lima, Peru). J. Mech. Behav. Biomed. Mater. 111, 104023.
Greisler, H.P., Schwarcz, T.H., Ellinger, J., Kim, D.U., 1986. Dacron inhibition of arterial regenerative activities. J. Vasc. Surg. 3 (5), 747–756.
Gui, L., Muto, A., Chan, S.A., Breuer, C.K., Niklason, L.E., 2009. Development of decellularized human umbilical arteries as small-diameter vascular grafts. Tissue engineering. Part. Accel. 15 (9), 2665–2676.
Gui, L., Boyle, M.J., Kamin, Y.M., Huang, A.H., Starcher, B.C., Miller, C.A., et al., 2014. Construction of tissue-engineered small-diameter vascular grafts in fibrin scaffolds in 30 days. Tissue Eng. 9–10, 1499–1507.
Helms, F., Lau, S., Aper, T., Zippusch, S., Klingenberg, M., Haverich, A., et al., 2021a. A 3-layered bioartificial blood vessel with physiological wall architecture generated by mechanical stimulation. Ann. Biomed. Eng.
Helms, F., Haverich, A., Böer, U., Wilhelmi, M., 2021b. Transluminal compression increases mechanical stability, stiffness and endothelialization capacity of fibrin-based bioartificial blood vessels. J. Mech. Behav. Biomed. Mater. 124, 104835.
Helms, F., Lau, S., Klingenberg, M., Aper, T., Haverich, A., Wilhelmi, M., et al., 2020. Complete myogenic differentiation of adipogenic stem cells requires both biochemical and mechanical stimulation. Ann. Biomed. 48 (3), 913–926.
Helms, F., Zippusch, S., Aper, T., Kalies, S., Heisterkamp, A., Haverich, A., et al., 2022. Mechanical stimulation induces vasa vasorum capillary alignment in a fibrin-based tunica adventitia. Tissue Eng.
Hennecke, K., Redeker, J., Kuhbier, J.W., Strauss, S., Allmeling, C., Kasper, C., et al., 2013. Bundles of spider silk, braided into sutures, resist basic cyclic tests: potential use for flexor tendon repair. PLoS One 8 (4), e61100.
Isenberg, B.C., Williams, C., Tranquillo, R.T., 2006. Endothelialization and flow conditioning of fibrin-based media-equivalents. Ann. Biomed. Eng. 34 (6), 971–985.
Konig, G., McAllister, T.N., Dusserre, N., Garrido, S.A., Iyican, C., Marini, A., et al., 2009. Mechanical properties of completely autologous human tissue engineered blood vessels compared to human saphenous vein and mammary artery. Biomaterials 30 (8), 1542–1550.
Koop, F., Strauß, S., Peck, C., Aper, T., Wilhelmi, M., Hartmann, C., et al., 2022. Preliminary application of native Nephila edulis spider silk and fibrin implant causes granulomatous foreign body reaction in vivo in rat's spinal cord. PLoS One 17 (3), e0264486.
Kuhbier, J.W., Reimers, K., Kasper, C., Allmeling, C., Hillmer, A., Menger, B., et al., 2011. First investigation of spider silk as a braided microsurgical suture. J. Biomed. Mater. Res. B Appl. Biomater. 97 (2), 381–387.
Kuhbier, J.W., Coger, V., Mueller, J., Liebsch, C., Schlottmann, F., Bucan, V., et al., 2017a. Influence of direct or indirect contact for the cytotoxicity and blood compatibility of spider silk. J. Mater. Sci. Mater. Med. 28 (8), 127.
Kuhbier, J.W., Coger, V., Mueller, J., Liebsch, C., Schlottmann, F., Bucan, V., et al., 2017b. Influence of direct or indirect contact for the cytotoxicity and blood compatibility of spider silk. J. Mater. Sci. Mater. Med. 28 (8), 127.
Lau, S., 2017. Strategies for the Generation of Fully Autologous Tissue-Engineered Fibrin-Based Vascular Grafts Resembling Three-Layered Natural Arteries.
Liebsch, C., Bucan, V., Menger, B., Köhne, F., Waldmann, K., Vaslaitis, D., et al., 2018. Preliminary investigations of spider silk in wounds in vivo - implications for an innovative wound dressing. Burns 44 (7), 1829–1838.
Liebsch, C., Fliess, M., Kuhbier, J.W., Vogt, P.M., Strauss, S., 2020. Nephila edulis-breeding and care under laboratory conditions. Dev. Gene. Evol. 230 (2), 203–211.
Radtke, C., Allmeling, C., Waldmann, K., Reimers, K., Thies, K., Schenk, H.C., et al., 2011. Spider silk constructs enhance axonal regeneration and remyelination in long nerve defects in sheep. PLoS One 6 (2), e16990.
Rising, A., Nimmervoll, H., Grip, S., Fernandez-Arias, A., Storckenfeldt, E., Knight, D.P., et al., 2005. Spider silk proteins–mechanical property and gene sequence. Zool. Sci. (Tokyo) 22 (3), 273–281.
Roll, S., Muller-Nordhorn, J., Keil, T., Scholz, H., Eidt, D., Greiner, W., et al., 2008. Dacron.sup.[R] .sup.vs. PTFE as bypass materials in peripheral vascular surgery - systematic review and meta-analysis. BMC Surg. 8, 22.
Rousou, J.A., 2013. Use of fibrin sealants in cardiovascular surgery: a systematic review. J. Card. Surg. 28 (3), 238–247.
Salehi, S., Koeck, K., Scheibel, T., 2020. Spider silk for tissue engineering applications. Molecules 25 (3), 737.
Shaikh, F.M., Callanan, A., Kavanagh, E.G., Burke, P.E., Grace, P.A., McGloughlin, T.M., 2008. Fibrin: a natural biodegradable scaffold in vascular tissue engineering. Cells Tissues Organs 188 (4), 333–346.
Soletti, L., Hong, Y., Guan, J., Stankus, J.J., El-Kurdi, M.S., Wagner, W.R., et al., 2010. A Bi-layered elastomeric scaffold for tissue engineering of small-diameter vascular grafts. Acta Biomater. 6 (1), 110–122.
Strauß, S., Reimers, K., Allmeling, C., Kuhbier, J.W., Radtke, C., Schäfer-Nolte, F., et al., 2013. Spider silk - a versatile biomaterial for tissue engineering and medical applications. Biomed. Tech. 58 (Suppl. 1).
Tai, N.R., Salacinski, H.J., Edwards, A., Hamilton, G., Seifalian, A.M., 2000. Compliance properties of conduits used in vascular reconstruction. Br. J. Surg. 87 (11), 1516–1524.
Tu, J.V., Pashos, C.L., Naylor, C.D., Chen, E., Normand, S.L., Newhouse, J.P., et al., 1997. Use of cardiac procedures and outcomes in elderly patients with myocardial infarction in the United States and Canada. N. Engl. J. Med. 336 (21), 1500–1505.
Vollrath, F., 2000. Strength and structure of spiders' silks. J. Biotechnol. 74 (2), 67–83.
Wilhelmi, M., Jockenhoevel, S., Mela, P., 2014. Bioartificial fabrication of regenerating blood vessel substitutes: requirements and current strategies. Biomed. Tech. 59 (3), 185–195.
Young, R.J., Holland, C., Shao, Z., Vollrath, F., 2021. Spinning conditions affect structure and properties of Nephila spider silk. MRS Bull. 46 (10), 915–924.
Zhang, Q., Li, M., Hu, W., Wang, X., Hu, J., 2021. Spidroin-based biomaterials in tissue engineering: general approaches and potential stem cell therapies. Stem Cell. Int. 2021, 7141550.